Corrosion Science 50 (2008) 3329–3335

Contents lists available at ScienceDirect

Corrosion Science

journal homepage: www.elsevier.com/locate/corsci

Cathodic protection of steel in concrete using magnesium alloy anode

G.T. Parthiban [a,*], Thirumalai Parthiban [a], R. Ravi [a], V. Saraswathy [a], N. Palaniswamy [a], V. Sivan [b]

[a] Central Electrochemical Research Institute, Karaikudi 630 006, India
[b] National Institute of Technology, Trichirappalli, India

ARTICLE INFO

Article history:
Received 13 February 2007
Accepted 5 August 2008
Available online 31 August 2008

Keywords:
A. Steel
A. Concrete
A. Magnesium anode
C. Corrosion
C. Cathodic protection

ABSTRACT

Corrosion of steel embedded in concrete structures and bridges is prevented using cathodic protection. Majority of the structures protected employ impressed current system. Use of sacrificial system for the protection of steel in concrete is not as widely employed. The use of magnesium anodes for the above purpose is very limited. This study has been carried out with a view to analyse the use of magnesium alloy anode for the cathodic protection of steel embedded in concrete.

Magnesium alloy anode, designed for three years life, was installed at the center of reinforced concrete slab, containing 3.5% sodium chloride with respect to weight of cement, for cathodic protection. Potential of the embedded steel and the current flowing between the anode and the steel were monitored, plotted and analyzed. Chloride concentration of concrete at different locations, for different timings, were also determined and analyzed.

The magnesium anode was found to shift the potential of the steel to more negative potentials initially, at all distances and later towards less negative potentials. The chloride concentration was found to decrease at all the locations with increase in time. The mechanism of cathodic protection with the sacrificial anode could be correlated to the removal of corrosive ions such as chloride from the vicinity of steel.

1. Introduction

The corrosion of the embedded steel leads to the deterioration of concrete structures and reduction in their durability. Studies on the corrosion of the embedded steel show that the corrosion products formed on the steel surface generate tensile stresses as high as 490 MPa, on the surrounding concrete [1–3].

Chloride ions are reported to be mainly responsible for the corrosion of steel embedded in concrete resulting in deterioration of concrete [4–14]. This leads to unanticipated, premature failure of concrete structures with considerable impact on economy and the society. Hence it is of utmost importance to prevent the corrosion of steel embedded in concrete.

Among the various corrosion control methods available, cathodic protection is a major technique adopted to control the corrosion of steel embedded in concrete [15–23]. Cathodic protection system is aimed to shift the potential of the steel to the least probable range for corrosion. Cathodic protection effectively stops the corrosion process and has been determined by the Federal Highway Administration to be the only rehabilitation technique able to prevent further corrosion in such structures regardless of the salt content in concrete. Hence, Federal Highway Administration, USA has declared that cathodic protection is the most effective technique that can stop the corrosion of the steel embedded in concrete [24,25]. The American Concrete Institute (ACI), AASHTO-AGC-ARTBA Task Force 29, and the National Association of Corrosion Engineers (NACE International) have also endorsed cathodic protection for reinforced concrete structures. As a result, cathodic protection for concrete using impressed current system is widely employed [26–38].

Cathodic protection must be properly monitored and maintained to ensure its effectiveness. It is established that among the various electrochemical methods, the increasingly used field technique for detecting corrosion activity in embedded steel is that of potential measurement [39–43].

Sacrificial anodes have the advantage that they require no auxiliary power supply. They can be used for prestressed or post tensioned concrete without the risk of increased potential shifts which might lead to hydrogen embrittlement of the steel. Also, since the anode is directly connected to the steel, electrical shorting is of no concern. Arc sprayed zinc with thickness ranging from 300 to 400 μm was evaluated by several researches [44–50]. The reaction products formed by the anode at the anode/concrete interface have resulted in disturbing the electrical continuity. Further, when the concrete is relatively dry, the current output considerably decreased with time due to passivating effects of the $ZnO/Zn(OH)_2$ formed. These would result in insufficient current to maintain the cathodic protection. Aluminium alloys containing Zn and In were also studied for their use as submerged anodes [51–53]. Here

* Corresponding author.
E-mail address: thirumalaip@yahoo.com (G.T. Parthiban).

0010-938X/$ - see front matter © 2008 Elsevier Ltd. All rights reserved.
doi:10.1016/j.corsci.2008.08.040

again, the oxidation products formed at the sacrificial anode/concrete interface led to the sharp decline in anode current output with time. Concrete being a high resistivity environment, requires anodes with higher driving voltage. Therefore, the use of magnesium anodes is favorable. However studies on the use of magnesium alloy sacrificial anodes for cathodic protection in concrete are very limited [54,55]. These studies indicated that longer durations are required for the cathodic protection to stabilize. In addition, long term performance of the magnesium anode for protection of steel in concrete needs to be established. Hence, this paper concentrates on evaluating the long term performance of Mg anode for cathodically protecting the steel embedded in concrete.

2. Experimental

2.1. Concrete slab

Ordinary Portland cement was used for casting slabs of size 1.6 m × 1.6 m × 0.1 m. The sand, used as fine aggregate, and 0.02–0.03 m sized coarse aggregate were washed thoroughly with de-ionized water, to remove any ionic contaminants, prior to their usage. The mix ratio used was 1:1.5:3, with water/cement ratio of 0.45. Sodium chloride, equivalent to 3.5% by weight of cement, was dissolved in the water used for casting.

0.01 m diameter and 1 m long steel rods were cleaned with inhibited pickling solution and thoroughly washed and dried. Two mats of the reinforcement were assembled, one for the top mat and the other for bottom mat with provision for fixing the anode at the center. The two mats were joined at diagonally opposite ends by vertical steel rods (of the same material) by welding. The surface area of the reinforcement assembly to be protected was 1.263 m^2.

A cylindrical empty space of diameter 0.30 m and depth of 0.08 m was provided at the center of the slab, during casting, for plugging the anode. Each steel rod was provided with wire connections, to extend outside the slab. The assembly was embedded in the concrete with a cover thickness of 0.025 m for both the top and bottom mats.

Rows and columns of points, paralleling the embedded reinforcement, were marked on the slab surface, where the potential measurements were made. A 0.0125 m deep pond was provided at the top for regularly wetting the slab with triple distilled water.

2.2. Cathodic protection

The potential of the embedded steel was measured at the various points after 23 h of casting the slab. Copper/copper sulphate electrode was used as the reference electrode.

The total surface area of the steel to be protected was estimated to be 1.263 m^2. A high purity magnesium alloy anode was chosen for the study. The composition of the anode was determined with Thermo EDAX unit. The anode was designed for a life of three years. A 0.008 m diameter and 0.3 m long steel core was provided at the center of the anode. It was packed in conventional backfill (75% gypsum, 20% bentonite clay, and 5% sodium sulfate) and plugged into the central hole provided in the slab. The open circuit potential of the anode was measured at different points on the concrete surface adjacent to the backfill.

Cathodic protection was applied by connecting the anode with the steel rods at the diagonal ends of the slab through switching units. The potential of the embedded steel at different distances from the anode and the current flowing in the circuit was measured after 1, 2, 3, 4, 24, 48, 72, 96, 144, 192 h and later periodically, when the cathodic protection current was on. The potentials at different distances from the anode were plotted against the time of measurement. The current measured was also plotted against the time of measurement. These were analyzed to understand the influence of magnesium anode on the protection offered to the embedded steel.

Fig. 1. Cathodically protected chloride contaminated concrete slab with magnesium alloy anode plugged at the center.

Fig. 1 illustrates the reinforced concrete slab with the anode placed at the center of the slab.

2.3. Chloride monitoring

Core drills of 0.01 m were obtained at three different distances from anode, at different durations, as close to the reinforcement assembly as possible. The core drills obtained were cut into five equal pieces, marking them from top to bottom corresponding to their location in the slab. Each piece was finely powdered to pass 300 μm mesh. The powder was digested for 24 h with de-ionized water and filtered with vacuum filtration unit. The clear solution was analyzed for its water soluble chloride content, since it is reported that the corrosion of the steel reinforcement is promoted by the chloride that is free to diffuse in the bulk of the concrete [56,57].

Also, after the test duration, the backfill samples were obtained from different locations adjacent to the anode. These samples were tested for their chloride content to understand the removal of chloride from concrete. 1 g of sample was digested for 24 h, in 100 cc of de-ionized water and filtered. The clear solution was titrated against standard silver nitrate solution, to determine its chloride content.

2.4. Tensile testing

To ascertain that the steel reinforcement was protected on embedding in the cathodically protected, chloride contaminated concrete, tensile testing was done for the reinforcement before embedding in the chloride contaminated concrete, using INSTRON 1195 universal testing machine. Tensile testing was also done for the reinforcement after retrieval from the cathodically protected slab, after 36 months. Specimens of 0.01 m diameter and 0.15 m length were use for testing. The load bearing capacity (load corresponding to yield strength) of the unexposed rod and the tested rod were compared to determine the extent of corrosion protection offered to the embedded rod.

3. Results and discussion

The magnesium alloy anode, having a composition of 0.184% manganese, 0.0053% iron, <0.005% other impurities and balance

magnesium, was employed for cathodically protecting the embedded steel. It had a diameter of 0.225 m and a length of 0.06 m with a weight of 4.2 kg (excluding weight of core). The anode exhibited an open circuit potential of −1.2549 ± 0.026 V (vs. $Cu/CuSO_4$) on the concrete surface adjacent to the backfill. It had a consumption rate of 1269 ± 16 kg/A. Yr in saturated calcium sulphate + saturated magnesium hydroxide with 0.1% chloride.

The interpretation of potential readings of reinforcement steel in concrete is most widely adopted since potential measurements form the basis of indicating the effectiveness of corrosion prevention. The regulations of ASTM C 876-91 (1999) and the interpretation in the offshore technology report (OTR), primarily indicate whether or not a structure is actively corroding and the areas where this activity is greatest based on potential of the embedded steel [58,59]. The potential of steel and the probability for corrosion reported by ASTM C 876 and OTR are given below:

ASTM C 876		OTR	
Potential (V vs. $Cu/CuSO_4$)	Probability for corrosion	Potential (V vs. $Cu/CuSO_4$)	Probability for corrosion (%)
<−0.350	>90%	−0.350 to −0.500	>95
−0.200 to −0.350	Uncertain	−0.200 to −0.350	~50
>−0.200	>90% no corrosion	>−0.200	<5

In this study, the magnesium alloy was galvanically coupled to the steel in concrete. Due to the inherent difference in EMF, the magnesium alloy is rendered as the anode and the steel becomes the cathode. Based on the above, the potentials measured in the concrete slabs, on coupling the embedded steel in concrete with the more active magnesium anode are presented and discussed.

Fig. 2 illustrates the variation in the potential of the embedded steel, at different timings, at a distance of 0.16 m from the magnesium alloy anode. Initially, the potential of the embedded steel at this distance was in the '90% corrosion' range as per ASTM C 876. The potentials ranged from −0.474 to −0.509 V (vs. $Cu/CuSO_4$), prior to the application of cathodic protection, at all points corresponding to this distance. When the potential was measured 1 h after the application of cathodic protection, the potential values at different points corresponding to this distance showed considerable shift. The shift in potentials ranged from 0.697 to −0.741 V. Even though these values are in the more negative range, the corrosion of the embedded steel would be negligible since it has been

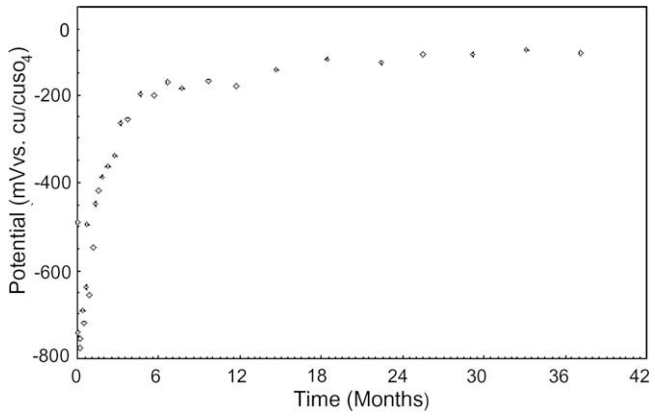

Fig. 2. Variation in potential of steel in concrete with time, on application of cathodic protection, at 0.16 m from anode.

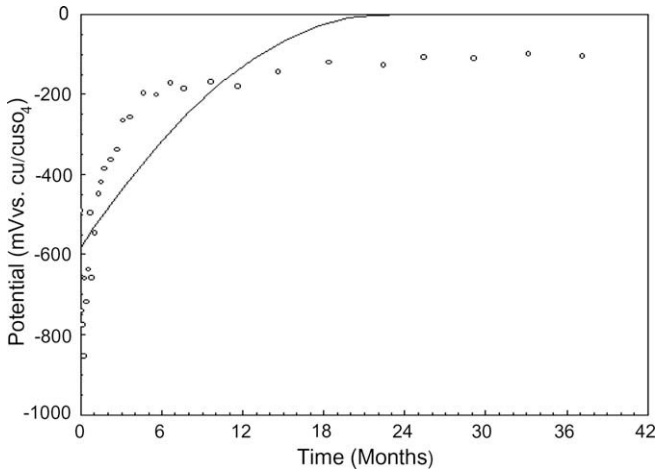

Fig. 3. Variation in potential of steel embedded in concrete as a second order function of time, at 0.16 m from anode.

rendered as the cathode [60]. With increase in time, the potentials shifted to less negative values.

This potential–time curve was analyzed using different mathematical equations to determine the best fit. Hence, different equations for the above trend were analyzed and the correlation coefficient was determined.

Fig. 3 illustrates the results of the analysis carried out using the equation

$$E = at^2 + bt + c$$

where a, b and c are constants. This analysis yielded the following equation for the curve-fit with a correlation coefficient of 0.7327:

$$E = -1.13228t^2 + 51.3621t - 582.12472$$

where E is the potential (V vs. $Cu/Cu\ SO_4$) and t is the time (month).

It is seen from the curve that deviations of the data points from the predicted curve are considerable. Hence, other possible equations were analyzed to identify the best fit.

Fig. 4 illustrates the results of the analysis carried out using the equation

$$E = a - b\ln(t + c)$$

where a, b and c are constants. This analysis yielded the following equation for the curve-fit with a correlation coefficient of 0.8302:

$$E = -583.6773 - 161.5302\ln(t + 0.5)$$

where E is the potential (V vs. $Cu/Cu\ SO_4$) and t is the time (month).

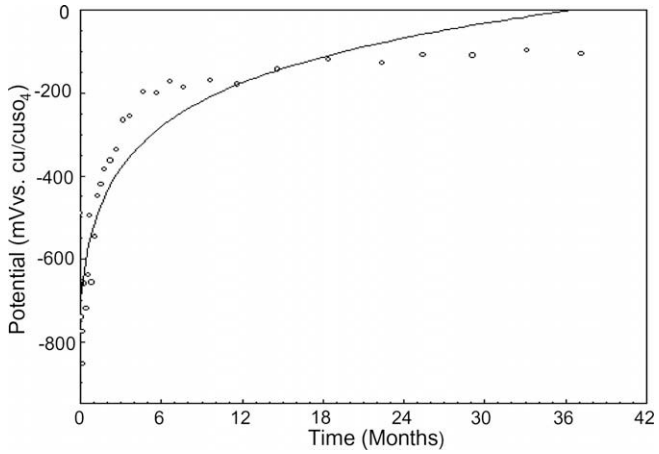

Fig. 4. Variation in potential of steel embedded in concrete as a logarithmic function of time, at 0.16 m from anode.

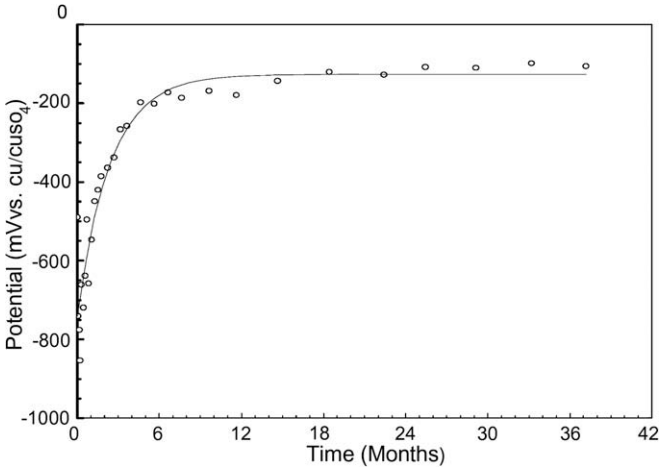

Fig. 5. Variation in potential of steel embedded in concrete as an exponential function of time, at 0.16 m from anode.

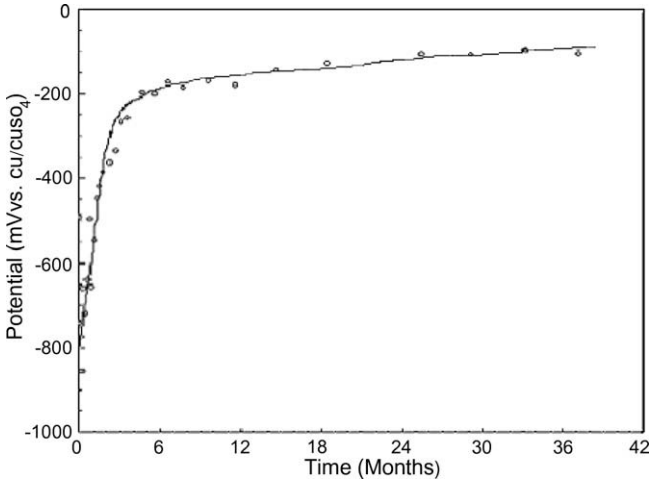

Fig. 6. Variation in potential of steel embedded in concrete as a sixth order function of time, at 0.16 m from anode.

It is seen from the curve that deviations of the data points from the predicted curve are still considerable. The deviation obtained is relatively very high. Hence, other possible equations were analyzed to identify the best fit.

Fig. 5 illustrates the results of the analysis carried out using the equation

$$E = a + b\mathrm{e}^{-kt}$$

where a and b are constants. This analysis yielded the following equation for the curve-fit with a correlation coefficient of 0.9211:

$$E = -127.0512 - 612.3097\mathrm{e}^{-0.4084t}$$

where E is thepotential (V vs. Cu/Cu SO_4) and t *is the time (month).* It is seen from the curve that deviations of the data points from the predicted curve are much reduced. Still, other possible equations were analyzed to identify a more possible best fit.

Among the various mathematical models analyzed for this system, the following equation exhibited the highest correlation coefficient of 0.9527, which is shown in Fig. 6.

$$E = -0.00002083t^6 + 0.00262t^5 - 0.12873t^4 + 3.1326t^3 - 39.2154t^2 + 240.2217t - 739.3582$$

where, E is the potential (V vs. Cu/Cu SO_4) and t is the time (month).

Among the different mathematical models analyzed, the above equation presented the best fit with minimum deviation. Time data were chosen to evaluate the accuracy for prediction with the above equation and the corresponding potential data were analyzed with respect to the predicted and measured values. The predicted values and the measured values of the potential of the embedded steel at different corresponding times are presented in Table 1.

The predicted value is observed to exhibit a deviation of 0.0336 V from the measured value, initially. As time increases, this deviation reduces to 0.0085 V. These deviations are relatively less significant as the measurements are made in concrete medium which inherently has very high resistivity. Hence the equation is observed to be highly accurate.

The variation in the potential of the embedded steel at different timings, at a distance of 0.50 m from the anode is shown in Fig. 7. Here also, the potential of the embedded steel was in the '90% corrosion' range, initially. Prior to the application of cathodic protection, the potentials ranged from −0.487 to −0.509 V, at all points corresponding to this distance. When the potential was measured 1 h after the application of cathodic protection, the potential values at different points corresponding to this distance showed considerable shift. Even though the potentials ranged from −0.508 to −0.537 V, the corrosion of the embedded steel would be negligible since it has been rendered as the cathode. With increase in time, the potentials shifted to less negative values and were >−0.2 V, after nearly three and a half months. The potential–time curve was analyzed with different equations. The following equation is

Table 1
Comparison of predicted and measured values of the potential of the embedded steel, at 0.16 m from the anode, with increase in time

Time (month)	Potential (V vs. Cu/$CuSO_4$)	
	Predicted	Measured
1.53	−0.4531	−0.4195
2.70	−0.3215	−0.3378
3.65	−0.2539	−0.2575
7.63	−0.1706	−0.1861
18.40	−0.1195	−0.1244
25.40	−0.0995	−0.1080

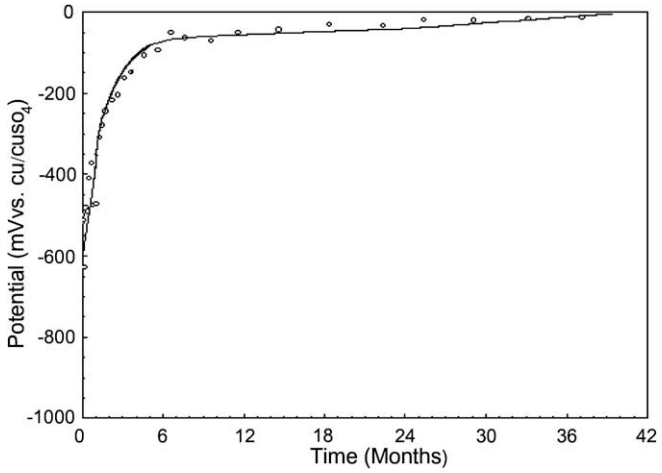

Fig. 7. Variation in potential of steel in concrete with time, on application of cathodic protection, at 0.50 m from anode.

found to be obeyed with the highest correlation coefficient of 0.9456:

$$E = -0.00001573t^6 + 0.002t^5 - 0.0995t^4 + 2.4643t^3 - 31.6335t^2 + 200.3296t - 553.0845$$

At a distance of 0.95 m from the anode, the variation in the potential of the embedded steel, at different timings, is illustrated in Fig. 8. Initially, the potential of the embedded steel at this distance was in the '90% corrosion' range. At all the points corresponding to this distance, the potentials ranged from −0.449 to −0.472 V, prior to the application of cathodic protection. When the potential was measured 1 h after the application of cathodic protection, the potential values at different points corresponding to this distance were shifted to the range −0.473 to −0.489 V. Here again, the corrosion of the embedded steel would be negligible since it has been rendered as the cathode. The potentials shifted to less negative values as time increased. Ultimately, the potentials shifted to >−0.2 V, after nearly two months. On analyzing the potential–time curve with different equations, it is found to obey the following equation with the highest correlation coefficient of 0.9728:

$$E = -0.00001788t^6 + 0.0022t^5 - 0.1075t^4 + 2.5716t^3 - 31.7015t^2 + 192.7451t - 501.1100$$

In general, as time increased the concrete dried during curing and the potentials shifted towards less negative values. However, when the cathodically protected slabs were drenched by rain, within the first few weeks after application of cathodic protection, the polarization of the steel was relatively more fluctuating as compared with the later stages and the potentials shifted towards more negative values. The frequent wetting of the concrete by rains increased the conductivity of the concrete, resulting in increased current flow and hence considerable potential shift. When the slabs dried up after the rains, the potentials shifted towards less negative values again. Ultimately, the potentials at all distances shifted to values >−0.2 V.

At later stages, potential fluctuations are not significantly observed, even during the monsoon seasons as seen from the measured potentials. The rate at which the potentials shift to less negative values decreases at longer times. This is due to the extent of polarization achieved due to the proximity of the anode at nearer distances to the anode. However, the potentials still shifted towards less negative values, at all times of measurement, as the distance from the anode increases, during the design life of the anode. The shift in potential observed is similar to the pattern reported for chloride-free and chloride-contaminated concrete [61] and a case study [62] that is reported.

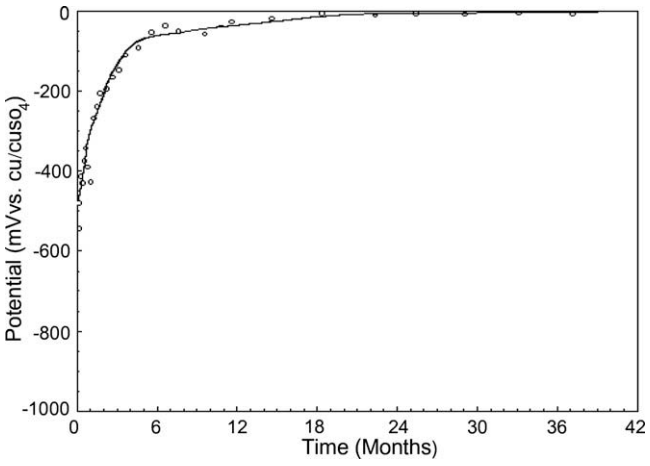

Fig. 8. Variation in potential of steel in concrete with time, on application of cathodic protection, at 0.95 m from anode.

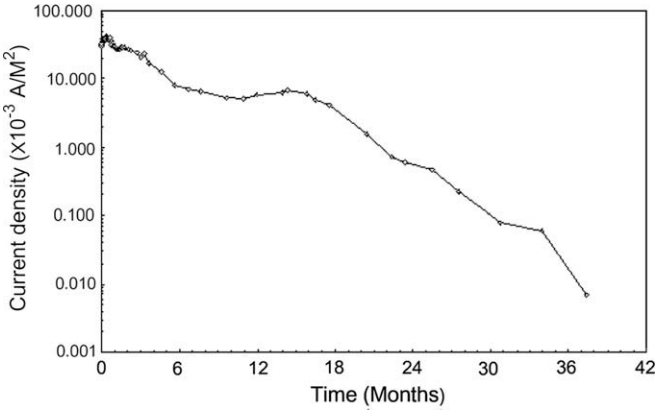

Fig. 9. Variation in current flowing in slab with time, on application of cathodic protection.

The shift in potential on application of cathodic protection and coefficients in the equations cited above are varying with distance from anode. These may be due to the distance from the anode and nature of porosity in the concrete corresponding to each distance which in turn would affect the resistivity/conductivity of the concrete for the corresponding distance.

The current flowing in the concrete during cathodic protection was also monitored periodically. The current densities measured at different durations are presented in Fig. 9. Here also, when the cathodically protected slabs were drenched by rain it shifted towards higher values, within the first few weeks after application of cathodic protection. During this period, the current flowing in the concrete was more fluctuating as compared with the later stages. Wetting of the concrete by the rains increased the conductivity of the concrete, resulting in considerable potential shift and hence increased current flow. When the slabs dried up after the rains, it shifted towards lesser values again. This could be due to the increase in the resistivity of the concrete. Other sacrificial systems investigated have reported lower initial current density values than those measured in the present work [49,54,63–65]. They also indicate that the current flowing in the system reduces with increase in time. In comparison, for an impressed current cathodic protection system applied to a bridge deck, the initial current required for the protection of steel in concrete ranges from 5 to 10 mA/m^2 of steel surface area [65,66] or about 25 mA/m^2 of concrete surface area [67]. The analysis of the current density–time curve, with different mathematical equations, yielded the following relationship with the highest correlation coefficient of 0.9459:

$$I = 1.4949 + 46.6441e^{-t/4.9495}$$

3.1. Effect of cathodic protection on chloride content

The shift in potential of the steel towards less negative values can be attributed to the chloride in the concrete being effectively leached away from the embedded steel, facilitating its passivation. The steel is reported to be in the immune zone with respect to corrosion, when its potential is less negative than −0.2 V for a chloride content less than 0.15% by weight of cement [66,68]. Hence, to understand the protection offered to the steel, the chloride content at different distances from the anode, at different times, was analyzed. The chloride contents in the proximity of the reinforcing steel at different timings, at three different distances from the anode were analyzed. The chloride content exhibited very little

variation in all the five sections of the core drill (from top to bottom) obtained from a location, at a specific duration. Hence, for each core drill, the chloride content was averaged for the five sections and reported.

At a distance of 0.23 m, the chloride content decreased rapidly from 12 kg/m^3 to about 0.35 kg/m^3 within three months. Later the chloride content decreased at a much lower rate. The chloride content decreased rapidly from 12 kg/m^3 to about 0.15 kg/m^3 within three months at a distance of 0.52 m. At this distance also, further decrease in the chloride content occurred at a much lower rate later. At a distance of 0.95 m, the chloride content decreased rapidly from 12 kg/m^3 to about 0.069 kg/m^3 within three months. Here again, the chloride content decreased at a much lower rate later. Table 2 gives the chloride (soluble) content of concrete determined at different distances from anode at different durations.

Comparison of the chloride content values with those reported, confirms that the steel is protected, reinforcing the inference based on corresponding potential shifts.

The backfill samples, obtained from different locations adjacent to the anode contained chloride equivalent to 0.2714 ± 0.031 kg/m^3. This indicates that considerable amount of chloride has been removed from the concrete. Since the slab was exposed to open atmosphere throughout the test duration, it is highly possible that the chloride could have been washed away by rains. Similar incidences of removal of chloride by washing away by rains are reported by other researchers as well [69].

3.2. Tensile behaviour

The load bearing capacities (load corresponding to yield strength) of the steel rods before and after test are presented in Table 3. Comparison of the values of the untested and tested rods indicates that the tested rods have undergone very little reduction in their load bearing capacity, only about 3%, and hence in their cross-section. The steel, retrieved from the cathodically protected concrete was subjected to longer pickling durations for cleaning. The observed reduction in the load and hence the cross-section could be partially due to the above fact as well. Hence, it can be inferred that the embedded steel was effectively cathodically protected by the magnesium alloy anode during the test period.

After the test duration, the anodes were removed from the slabs, cleaned and weighed. The anodes had undergone 79.185 ± 2.011% weight loss after the test period. The efficiency of the anode could not be determined since the current flow was not constant.

Table 2
Variation of chloride (soluble) content in concrete, with distances from anode and time

	Soluble chloride content (kg/m^3)		
Distance from anode (m) →	0.23	0.50	0.95
Duration of cathodic protection (months) ↓			
0.00	12.0000	12.0000	12.0000
0.27	10.0000	8.5114	5.3703
0.56	6.0256	4.7252	3.1580
1.06	4.1687	2.6915	1.3804
2.17	0.6761	0.3302	0.1468
3.02	0.3585	0.1496	0.0693

Table 3
Comparison of yield load of unused and cathodically protected steel

Specimen	Yield load (kN)	
	Unused	Cathodically protected
1	122.57	119.98
2	125.11	123.69
3	129.23	121.74
Average	125.64	121.80

4. Conclusions

Cathodic protection of the embedded steel bar could be achieved in chloride contaminated concrete using magnesium alloy anode containing 0.184% manganese.

The potential of the embedded steel shifted from more negative values to less negative plateau, at all distances from the anode.

The current flowing in the concrete decreased with increase in time.

The concentration of chloride ions at different distances from anode decreased with increase in time on application of cathodic protection.

The shift in potential towards less negative values and the decrease in chloride content with time at any distance from anode confirmed the protection offered to the embedded steel.

The very small reduction in the yield load after the test duration further confirmed the protection offered to the steel embedded in the concrete.

References

[1] E.B. Rosa, B. McCollum, O.S. Peters, Electrolysis in Concrete, Paper No. 18, Bureau of Standards, Department of Commerce, Washington, DC, 1919.
[2] J.H. Hoke, C. Chama, K. Rosengarth, Measurement of stresses developing during corrosion of embedded concrete reinforcing bars, Corrosion '83, Paper No. 168, National Association of Corrosion Engineers, Houston, Texas, 1983.
[3] K. Hladky, D.G. John, J.L. Dawson, Development in Rate of Corrosion Measurements for Reinforced Concrete Structures, Corrosion '89, Paper No. 169, National Association of Corrosion Engineers, Houston, Texas, 1989.
[4] D. Whiting, Concrete materials, mix design, construction practices and their effects on the corrosion of reinforcing steel, Corrosion '78, Paper No. 73, NACE, Houston, Texas, 1978.
[5] H.A. Brodersen, Influence of the structure and composition of the cement stone upon the diffusion of ion in the concrete, Ph.D. Dissertation, Faculty for Architecture of the Technical Institute of Rhine Westfalia in Aachen, West Germany, 1982.
[6] Comite Euro-International Du Beton, Durability of concrete structures-State of the art Report, Bulletin O'Information Number 148, Paris, France, 1982.
[7] D.A. Lewis, Some aspects of the corrosion of steel in concrete, in: Proceeding of the First International Congress on Metallic Corrosion, London 547, 1962.
[8] H.A. Berman, The effects of sodium chloride on the corrosion of concrete reinforcing steel and on the pH of calcium hydroxide solution, Report No. FHWA-RD-74-1, Federal Highway Administration, Washington, DC, 1974.
[9] K.C. Clear, Time-to-corrosion of reinforcing steel in concrete slabs, Report No. FHWA-RD-76-70, Federal Highway Administration, Washington, DC, 1976.
[10] H. Arup, The mechanisms of the protection of steel by concrete, in: A.P. Crane (Ed.), Corrosion of Reinforcement in Concrete Construction, Ellis Horwood Publishers, Chichester UK, 1983.
[11] C.L. Page, O. Vennesland, Pore solution composition and chloride binding capacity of silica fume and silica pastes, in: 2nd International Seminar on Electrochemistry on Corrosion of Steel in Concrete, Copenhagen, Denmark, 1982.
[12] A. Molina, M.T. Blanco, C. Andrade, Corrosion rate of three different types of galvanized coatings of steel reinforcement in contact with mortar, in: Proc. of 9th International Congress on Metallic Corrosion, 1, National Research Council of Canada, Ottawa, Canada, 1984.
[13] K. Pettersson, Cement Concr. Res. 20 (1994) 461.
[14] S.E. Hussain, A. Rasheeduzzafar, A. Al-Mussallam, A.S. Al-Gahtani, Cement Concr. Res. 25 (7) (1995) 1543.
[15] L. Bertolini, F. Bolzoni, A. Cigada, T. Pastore, P. Pedeferri, Corros. Sci. 35 (5–8) (1993) 1633.
[16] M. Mckenze, Research Report 328, Cathodic protection of reinforced concrete, Transport and Road research Laboratory, Department of Transport, Crowthorne, Berkshire, UK, 1991.
[17] K.M. Howell, Mater. Perform. 32 (8) (1993) 16.
[18] N.C. Webb, Constr. Build. Mater. 6 (3) (1992) 179.
[19] K.D. Phillips, Cathodic Protection of Reinforced Concrete Bridges, vol. 4, Published by NACE, Houston, TX, USA, 1985.
[20] J.B. Vrable, Cathodic Protection for Reinforced Concrete Bridge Decks, NCHRP Report 180, 1977.
[21] P.J. Jurach, An evaluation of the effectiveness of cathodic protection of seven bridge decks, California Department of Transportation, Report No. FHWA-DP34-2, 1982.
[22] W.R. Schutt, Practical experiences with bridge deck cathodic protection, Paper No. 74 presented at National Association of Corrosion Engineers, Corrosion 78, Houston, TX, 1978.

[23] H.C. Schell, D.G. Manning, K.C. Clear, Cathodic protection of bridge substructures burlington bay skyway test site, Initial Performance of Systems 1 to 4, Presented at 63rd Annual Transportation Research Board Meeting, Washington, DC, 1984.
[24] R.A. Barnhart, 'FHWA position on cathodic protection systems memorandum from FHWA to Regional and Federal Progress Administrations, 1982.
[25] J. Leggedoor, G.E. Schuten, in: Proceedings of the Conference on Solution to Corrosion Problem, EUROCORR 98, Event #221, Bidthoven, Netherlands, 191, 1998.
[26] I. Solomon, M.E. Bird, B. Phang, Corros. Sci. 35 (5–8) (1993) 1649.
[27] D.H. Hong, W.G. Fan, D.K. Luo, Y. Ge, Y.X. Zhu, ACI Mater. J. 90 (1) (1993) 3.
[28] H. Mcarthur, S. Darcy, J. Barker, Constr. Build. Mater. 7 (2) (1993) 85.
[29] R.B. Poler, P.C. Nuiten, Mater. Perform. 33 (6) (1994) 11.
[30] B.L. Martin, C.A. Finlotte, Mater. Perform. 34 (9) (1995) 26.
[31] R.P. Brown, J.S. Tinnea, Mater. Perform. 30 (8) (1991) 28.
[32] E. Mejia, E. Proverbio, O. Garcia, E. Traversa, Mater. Perform. 34 (8) (1995) 27.
[33] K. Takewaka, Corros. Sci. 35 (5–8) (1993) 1617.
[34] M.G. Ali, G.J. Alsulaimani, ACI Mater. J. 90 (1) (1993) 8.
[35] M.G. Ali, ACI Mater. J. 90 (3) (1993) 247.
[36] C.L. Page, Sergi, D. Thomson, Mater. Struct. 24 (143) (1991) 359.
[37] W.H. Hartt, C.C. Kumria, R.J. Kessler, Corrosion 49 (5) (1993) 377.
[38] B. Bazzoni, L. Lazzari, Mater. Perform. 31 (12) (1992) 13.
[39] R. Stratfull, Mat. Perform. 7 (3) (1968) 29.
[40] J.P. Broomfield, J.S. Tinnea, Field survey of cathodic protection on North American bridges, Report No. SHRP-C/UWP-92-618, (1993).
[41] J.Bennett, T.Turk, Technical alert–Criteria for the cathodic protection of reinforced concrete bridge elements, Report No. SHRP-S-359, Strategic Highway Research Program, Washington, DC, 1994.
[42] L. Bertolini, P. Pedeferri, T. Pastore, B. Bazzoni, L. Lazzari, Corrosion 52 (7) (1996) 552.
[43] RP 0100-2004, Cathodic Protection of Prestressed Concrete, NACE, Houston, TX, 2004.
[44] J.A. Apostolos, D.M. Parks, R.A. Carello, Cathodic protection of reinforced concrete using metallized zinc, Paper #137, Corrosion '87, NACE, Houston, TX, 1987.
[45] B.S. Covino, S.J. Bullard, G.R. Holcomb, S.D. Cramer, G.E. Mc Gill, C.B. Cryer, Electrochemically aged arc sprayed Zn coatings on concrete, Paper #308, Corrosion '96, NACE, Houston, TX, 1996.
[46] R.J. Kessler, R.G. Powers, I.R. Lasa, Zn metallizing for galvanic CP of steel reinforced concrete in marine environment, Paper #324, Corrosion '90, NACE, Houston, TX, 1990.
[47] M. Funahashi, W.T. Young, Development of new sacrificial anode for reinforced and prestressed concrete, in: II CANMET/ACI International Symposium on advances in concrete technology, Las Vegas, 1995.
[48] J. Broomfield, R. Brousseau, M. Arnott, B. Baldock, Mater. Prot. 34 (1) (1994) 40.
[49] A.A. Sagues, R.G. Powers, Corrosion 52 (7) (1996) 508.
[50] O.T. de Rincor, M.F. de Romero, A.R. de Carruyo, M. Sanchez, J. Provo, Mater. Struct. 30 (1997) 556.
[51] L. Bertolini, M. Gastoldi, M. Pedeferri, E. Redaelli, Corros. Sci. 44 (2002) 1497.
[52] M. Funahashi, W.T. Young, Field Evaluation of New Aluminium Alloy Sacrificial Anode for Steel Embedded in Concrete, FHWA Publications, FHWA RD 98058, 1998.
[53] M. Funahashi, S.F. Daily, W.T. Young, Performance of newly developed sacrificial anode CP system, Paper #254, Corrosion '97, NACE, Houston, TX, 1997.
[54] R.J. Kessler, R.G. Powers, I.R. Lasa, Mat. Perform. 37 (3) (1998) 10.
[55] G.T. Parthiban, V. Saraswathy, N.S. Rengaswamy, Bull. Electrochem. 16 (6) (2000) 253.
[56] B.H. Oh, S.Y. Jang, Cement Concr. Res. 37 (2007) 47–53.
[57] B. Martin Perez, H. Zibara, R.D. Hooton, M.D.A. Thomas, Cement Concr. Res. 30 (2000) 1215–1223.
[58] ASTM C876-91: Standard Test Method for Half-Cell Potentials of Uncoated Reinforcing Steel in Concrete, ASTM International, West Conshohocken, PA, USA, 1999.
[59] Offshore technology report, Department of Energy: Development of inspection techniques for reinforced concrete, Concrete in the Oceans Series, HMSO, London, 1986.
[60] G.K. Glass, Mater. Perform. 35 (2) (1996) 36.
[61] P. Thirumalai, R. Ravi, Corros. Sci. 47 (2005) 1625.
[62] G.K. Glass, A.M. Hassanein, N.R. Buenfeld, Cathodic protection of steel in concrete, Report Submitted to Engineering and Physical Sciences Research Council, UK, 2001.
[63] R. Pangrazzi, W.H. Hartt, R. Kessler, Corrosion 50 (3) (1994) 186.
[64] R. Brousseau, B. Baldock, Corrosion 54 (3) (1998) 241.
[65] L. Bertolini, MariaPia Pedeferri, Matteo Gastaldi, Elena Redaelli, Corros. Sci. 44 (2002) 1497.
[66] J.P. Broomfield, Mater. Perform. 31 (9) (1992) 28.
[67] L. Bertolini, F. Bolzoni, P. Pedeferri, L. Lazzari, T. Pastore, J. Appl. Electrochem. 28 (1998) 1321.
[68] P. Pedeferri, L'Edilizia, XII 10 (1993) 69.
[69] P. Castro, O.T. De Rincon, E.J. Pazini, Cement Concr. Res. 31 (4) (2001) 529.